Escola de Primavera de Transição e Turbulência
Blumenau 2020

12th Spring School on Transition and Turbulence
September 21st-25th, 2020, Blumenau, SC, Brazil

EPTT-2020-0051
NUMERICAL INVESTIGATION OF WAVY LEADING EDGE EFFECTS ON DRAG AND LIFT COEFFICIENTS OF NACA 0015 AIRFOIL

João Victor Salvaro
Centro Universitário Católica de Santa Catarina
joao.salvaro@catolicasc.org.br

Gustavo Luiz Macedo da Silva
Centro Universitário Católica de Santa Catarina
gustavo.macedo@catolicasc.org.br

Fernando Almeida Rocha
Centro Universitário de Católica Santa Catarina
fernando.rocha@catolicasc.org.br

Abstract. *The wavy leading edge has been investigated as a flow control mechanism with the purpose of increasing aerodynamic performance. This study numerically investigated the effects on drag and lift caused by the A3λ11 wavy leading edge on a NACA 0015 wing. Simulations, using the k-ω SST turbulence model present in the Ansys Fluent library, were performed under* $Re = 6.8x10^4$ *using wings with* $MAC = 0{,}120\ m$ *and* $AR = 4{,}17$. *The modification increased* C_L/C_D *ratio by up to 41.3% and* $dC_L/d\alpha$ *by 20.7% in the pre-stall regime, reducing stall angle in 15.4%.*

Keywords: *Aerodynamics; CFD; Drag; Lift; Wavy leading edge*

1. INTRODUCTION

Recently, there has been great interest in researching geometric modifications in the leading edge as passive mechanisms in flow control; in particular, tubercles inspired on humpback whale's pectoral flippers (Fig. 1).

Figure 1. Humpback Whale

Watts and Fish (2001) conducted the first non-viscous simulations (panel method) with finite wing (aspect ratio AR = 2.04) equipped with a sinusoidal leading edge. The wavy profile showed 4.8% increase in lift, reduction in induced drag by 10.9% and increase of 17.6% in the lift to drag ratio, when compared to the smooth wing for 10º angle of attack. After this study, several publications were made through numerical and experimental studies.

Levshin et al. (2006) and Johari et al. (2007) conducted the first research to visually evaluate the effect of the sinusoidal leading edge geometry on aerodynamic performance for a NACA 63_4-021. Variations in amplitude have a greater influence on performance when compared to changes in wavelength. Tubercles with shorter amplitude (2.5% of chord) had similar characteristics of lift in the pre-stall regime. In the post-stall region, the same condition showed smoother stall. Hansen et al. (2009), De Paula (2016) and Rocha et al. (2018) showed that the A3λ11 configuration (3% chord amplitude, 11% chord wavelength) shows greater maximum lift and smoother stall behavior.

Rostamzadeh et al. (2017) used the SST γ-Re transition model in the uRANS context visualization of current lines and pressure distribution. Through numerical simulations, Serson et al. (2017) investigated protuberances on the leading edge of NACA 0012 profile for $1000 \leq Re \leq 50000$, reporting that the wavy effect depends on the Reynolds number, as well as previous experimental research (STANWAY, 2008; CUSTODIO et al., 2012; DE PAULA, 2016; ROCHA et al., 2018).

2. METHODOLOGY AND NUMERICAL VALIDATION

The wings of profile NACA 0015, with smooth and wavy leading edge (A3λ11), were simulated for $Re = 6{,}8x10^4$ with 4% turbulence intensity (ANSYS, 2009) for angle of attack from 0° to 22°. The wing is shown in Fig. 2. It is rectangular with mean aerodynamic chord (MAC) of 0,12 m, wingspan (Z) of 0,5 m, resulting in an aspect ratio of 4.17, similar to the value presented on the Embraer EMB-312 Tucano aircraft (VOGELAAR, 2008). The amplitude (A) and peak-to-peak distance (λ) are respectively 3% and 11% of MAC.

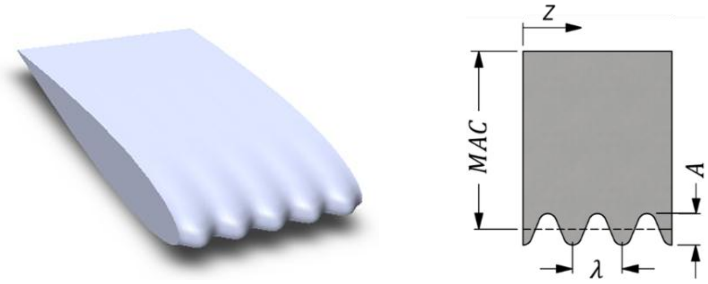

Figure 2. The wavy leading edge

The computational domain was modeled using the DesignModeler Geometry platform and based on the studies of ARAI et al. (2015). Inlet boundary was prescribed as constant speed fluid and is located five chords upstream from the wing leading edge. The airfoil was defined as static wall and centered between the lateral limits and the upper and lower limits, whose position is eight and ten chords away, respectively. The lateral faces were considered with symmetry conditions. The upper and lower limits of the control volume were defined as dynamics walls (with the same speed and direction of the fluid flow) to eliminate the non-slip condition. Finally, the domain depth was dimensioned with eight chords lengths and characterized with a constant gauge pressure. Then, the computational domain size was modeled with 15c x 10c x 8c (length x height x depth), as shown in Fig. 3.

The influence of the mesh refining on the lift and drag coefficients was verified. Through ANSYS Meshing, four configurations were generated about the smooth wing for analysis, as shown in Fig. 4. All of them have an unstructured character composed of tetrahedral elements.

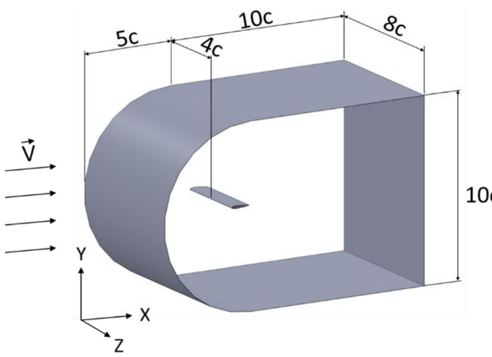

Figure 3. Computational domain

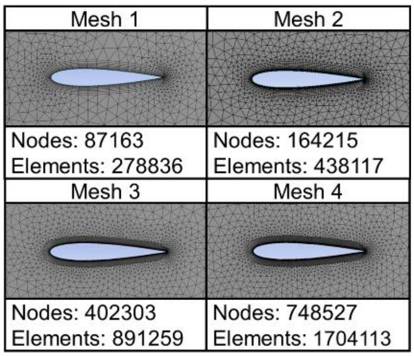

Figure 4. Mesh analysis

Table 1 shows the lift and drag coefficients obtained for the angle of attack α = 10°. This angle was adopted because it was noticed in the Tongsawang (2015) and Şahin and Acir (2015) literatures that α = 10° in low Reynolds numbers, is in a pre-stall region and has well-developed aerodynamic coefficients.

Aerodynamic coefficient	Meshes				Experimental
	Mesh 1	Mesh 2	Mesh 3	Mesh 4	
Lift	0.74	0.70	0.61	0.61	0.52
Drag	0.054	0.053	0.037	0.039	0.089

Table 1. Aerodynamic coefficients for α = 10°.

	Mesh 3	Mesh 4
Error CL (%)	16%	15%
Error CD (%)	53%	48%
Time (s)	2611	4656

Table 2. Mesh analysis.

Meshes 3 and 4 presented the values with greater precision in the lift coefficient, when compared to reality. This is justified by being the most refined. In the drag coefficient, these two meshes showed the most distant results from the experimental, while Mesh 1 was the best option.

In view of these results, criteria were developed to define which mesh (1, 3 or 4) would be more coherent for the next simulations in this study. The first criterion was to weigh the importance of each coefficient. It was noticed that in most aerodynamic airfoils studies the lift coefficient is more relevant than the drag. Therefore, the Mesh 1 that had presented the best values for the drag coefficient was discarded. The second criterion was based on the time and precision of the results obtained through the simulation, as shown in table 2.

The first line (Error CL (%)) shows the percentage difference between the numerical and experimental lift coefficient. Note that the errors of the two meshes are very similar. An analogous analysis can be performed for the second line (Error CD (%)), in which, it shows the percentage difference between the drag coefficients. This means that the results obtained between Meshes 3 and 4 were similar. Finally, the third line (Time (s)), which shows the simulation time of each mesh, showed the most significant difference. It is noticed that the simulation time with Mesh 3 is equivalent to approximately 56% of the simulation time with Mesh 4.

Based on these analyzes and being aware that the simulation time affects the computational cost, Mesh 3 was adopted as the configuration standard for the subsequent simulations. The wavy airfoil used a mesh with the same characteristics as the baseline model, however, due to its geometry, it has 912145 nodes and 1876967 elements.

Figure 5 compares the results of lift and drag (Curves C) with values presented by Şahin and Acir (2015) (Curves A and B). Note that the both curves C, referring to the smooth NACA 0015, present similar behavior to the experimental data ($dC_L/d\alpha$, $C_{L_{máx}}$, C_D and stall behavior), validating the simulations.

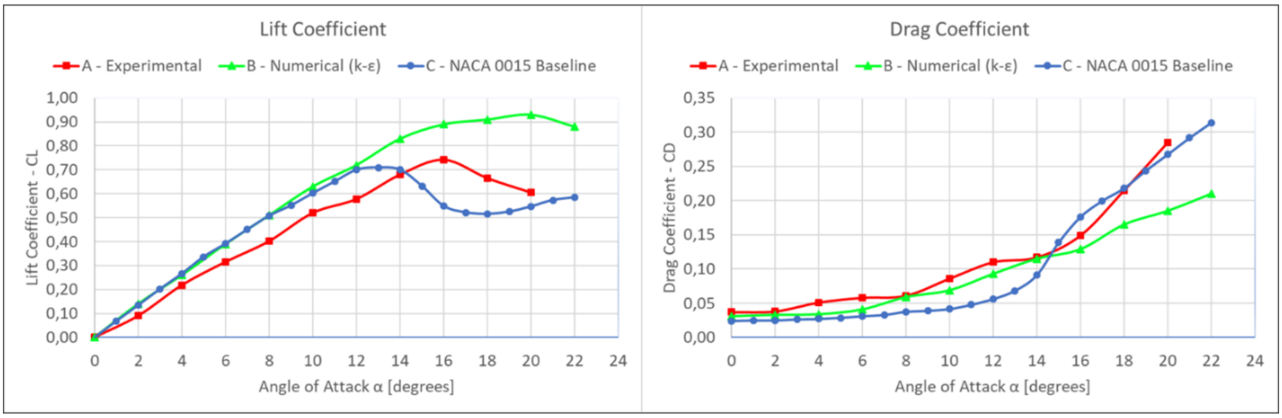

Figure 5. Aerodynamic coefficients for numerical validation

The k-ω SST turbulence model, which provides greater mesh refinement in the region close to the tubercles, was applied with the aim of facilitating convergence process.

3. RESULTS AND DISCUSSIONS

Figures 6 and 7 show the values of lift and drag coefficient, respectively, as a function of the angle of attack α for the smooth and wavy configurations. In the pre-stall regime, the modified profile showed a greater slope in lift coefficient curve (increase of 20.7%), similar value of maximum lift coefficient (smooth: $C_{L_{max}} = 0.709$, A3λ11: $C_{L_{max}} = 0.725$) and 15% reduction in the stall angle (smooth: $\alpha_{stall} = 13°$, A3λ11: $\alpha_{stall} = 11°$). In the post-stall regime, the modified wing presented a softer behavior than the smooth wing. The profiles showed a similar zero lift drag (smooth: $C_{D_0} = 0.0241$, A3λ11: $C_{D_0} = 0.0239$). This similarity was maintained until α = 8°, when the wavy model showed an increase in slope of the drag coefficient curve. In post-stall regime, the profiles showed similar drag coefficients.

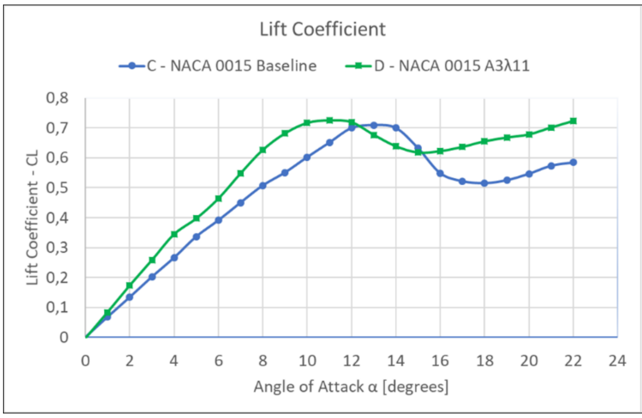

Figure 6. Lift Coefficient

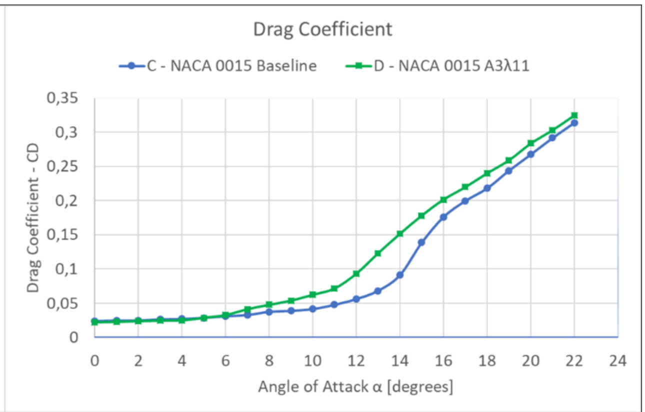

Figure 7. Drag Coefficient

Figure 8 shows that the aerodynamic efficiency (C_L/C_D) of the wing with wavy leading edge is greater between 0° to 6° and from 17° to 22°. At the lowest angles of attack, the increase in C_L/C_D ratio of A3λ11 profile is due to the greater growth of $dC_L/d\alpha$ and the similarity between the drag coefficients of the two airfoil models. At α = 4°, the aerodynamic efficiency of the modified configuration was 41.3% higher than the value obtained with the baseline.

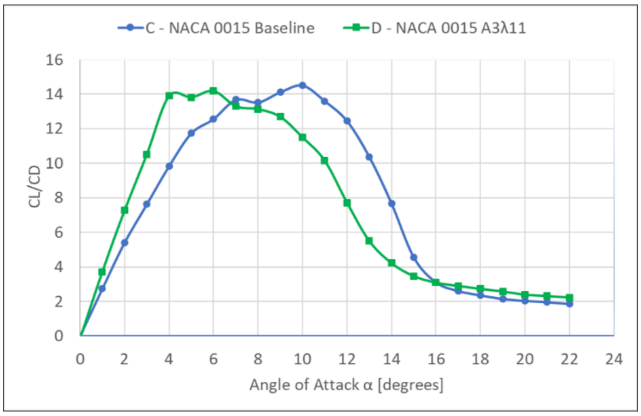

Figure 8. Aerodynamic coefficients for numerical validation

4. CONCLUSIONS

When compared to the smooth configuration in the pre-stall region, the NACA 0015 A3λ11 profile showed similar values for $C_{L_{max}}$ and C_{D_0}, in addition to the 15.4% reduction in stall angle. On the other hand, the modified configuration indicated increases of 20.7% in the $dC_L/d\alpha$ and 41.3% in aerodynamic efficiency. Finally, the wavy leading edge is shown as an efficient flow control mechanism in situations of low angle of attack and low Reynolds number, and could be applied in UAVs (Unmanned Aerial Vehicles).

5. REFERENCES

ANSYS, I. 7.3.2 Using Flow Boundary Conditions. 29 Jan. 2009. <https://www.afs.enea.it/project/neptunius/docs/fluent/html/ug/node238.htm>.

Arai, H.; Doi, Y.; Nakashima, T.; Mutsuda, H., 2015. *A Study on Stall Delay by Various Wavy Leading Edges.* Journal of Aero Aqua Bio-mechanisms, v. 1, p. 18-23.

Custodio, D.; Henoch, C.; Johari, H., 2012. *Aerodynamic characteristics of finite-span wings with leading edge protuberances.* Proceedings of the 50th AIAA Aerospace Science Meeting. Nashville, Tennessee: AIAA Paper 2012-0054.

De Paula, A. A., 2016. *The airfoil thickness effects on wavy leading edge phenomena at low Reynolds number regime*. Doctoral Thesis in Mechanical Engineering, University of São Paulo.

Hansen. K.L.; Kelso, R.M.; Dally, B.B.; Batill, S.M., 2009. *The effect of leading edge tubercle geometry on the performance of different airfoils*. Proceedings of the 7th World Conference on Experimental Heat Transfer, Fluid Mechanics and Thermodynamics, Krakow, Poland.

Johari, H.; Henoch. C.; Custodio, D.; Levshin, A., 2007. *Effects of leading-edge protuberances on airfoil performance.* AIAA Journal, v. 45, n. 11, p. 2634-2642.

Levshin, A., Custodio, D., Henoch, C., Johari, H., 2006. *Effects of Leading edge Protuberances on Airfoil Performance*. 36th AIAA Fluid Dynamic Conference And Exhibit.

Rocha, F.A.; De Paula, A.A.; Cavalieri, A.V.G.; Kleine, V. G.; Sousa, M.S., 2018. *Lift enhancement by wavy leading edges at Reynolds numbers between 700,000 and 3,000,000.* AIAA Aviation Forum, pp. 20.

Rostamzadeh, N., Kelso, R.M., Dally, B., 2017. *A Numerical Investigation into the Effects of Reynolds Number on the flow Mechanism Induced by a Tubercled Leading edge.* Theor. Comput. Fluid Dyn.

Şahin, İ.; Acir, A., 2015. *Numerical and Experimental Investigations of Lift and Drag Performances of NACA 0015 Wind Turbine Airfoil*. IJMMM, v. 3.

Serson, D., Meneghini J. R. and Sherwin, S. J., 2017. *Direct numerical simulations of the flow around wings with spanwise waviness*. Journal of Fluid Mechanics, v. 826.

Watts, P.; Fish, F.E., 2001. *The influence of passive, leading edge tubercles on wing performance*. Proceedings of the Twelfth International Symposium on Unmanned Untethered Submersible Technology, Durham New, Hampshire.

6. RESPONSIBILITY NOTICE

The authors are the only responsible for the printed material included in this paper.